

## **General Disclaimer**

### **One or more of the Following Statements may affect this Document**

- This document has been reproduced from the best copy furnished by the organizational source. It is being released in the interest of making available as much information as possible.
- This document may contain data, which exceeds the sheet parameters. It was furnished in this condition by the organizational source and is the best copy available.
- This document may contain tone-on-tone or color graphs, charts and/or pictures, which have been reproduced in black and white.
- This document is paginated as submitted by the original source.
- Portions of this document are not fully legible due to the historical nature of some of the material. However, it is the best reproduction available from the original submission.



# Application of Image Processing Technology to Problems in Manuscript Encapsulation

Final Report

D.L. Glackin  
E.P. Korsmo

(NASA-CR-173200) APPLICATION OF IMAGE  
PROCESSING TECHNOLOGY TO PROBLEMS IN  
MANUSCRIPT ENCAPSULATION Final Report (Jet  
Propulsion Lab.) 43 p HC A03/MF A01

N84-16528

Unclas

CSCL 14E G3/35 18215

September 15, 1983

Prepared for  
Los Angeles County Museum of Art  
Through an Agreement with  
National Aeronautics and Space Administrator  
by

Jet Propulsion Laboratory  
California Institute of Technology  
Pasadena, California

# Application of Image Processing Technology to Problems in Manuscript Encapsulation

Final Report

D.L. Glackin  
E.P. Korsmo

September 15, 1983

Prepared for  
Los Angeles County Museum of Art  
Through an Agreement with  
National Aeronautics and Space Administration  
by  
Jet Propulsion Laboratory  
California Institute of Technology  
Pasadena, California

The work described in this report was conducted by the Jet Propulsion Laboratory, California Institute of Technology, for the Los Angeles County Museum of Art, under an agreement with the National Aeronautics and Space Administration.



## ABSTRACT

In 1981, a famous sixteenth-century manuscript written by Leonardo da Vinci and owned by Dr. Armand Hammer was prepared for public display. The individual sheets were mounted between plexiglas and sealed. The long-term effects of the encapsulation technique were unknown at the time. The types of degradation of concern are (1) micro-burnishing, a rubbing off of the very fine surface texture by the plexiglas and (2) dimensional stressing of the manuscript by the response of the interior micro-climate to the exterior environment.

In order to study the problem, the manuscript was simulated with similar sheets of paper. They were photographed under repeatable raking-light conditions to enhance their surface texture, encapsulated in plexiglas, cycled in an environmental test chamber, and rephotographed at selected intervals. At JPL the film images were digitized, contrast-enhanced, geometrically registered, and apodized. An FFT analysis of a control sheet and two experimental sheets was performed to detect micro-burnishing. A difference image analysis was used to search for differential stretching.

The FFT analysis indicates no micro-burnishing. It reveals that the "mesoscale" deformations with sizes  $\sim 8\text{mm}$  are degrading monotonically, which is of no concern.

The difference image analysis indicates that the sheets were increasingly stressed with time and that the plexiglas did not provide a sufficient environmental barrier under the simulation conditions. The relationship of these results to the Codex itself is to be determined by LACMA.

## PREFACE

This report covers work performed by the Jet Propulsion Laboratory (JPL) Image Processing Applications and Development Section (384) for the Los Angeles County Museum of Art, Los Angeles, California. The JPL contract reference is Task Order No. RE-152/A341, Proposal No. 70-1862.

## ACKNOWLEDGMENTS

Technical discussions with Andy Collins and David Norris are gratefully acknowledged. Joe Fulton scanned the negatives. Thanks go to Dr. Ray Wall for his continued support. Special thanks are extended to James Druzik, William Leisher and Pieter Meyers of LACMA.

## DEFINITION OF ABBREVIATIONS

CDF	Cumulative Distribution Function
DN	Digital Number
FFT	Fast Fourier Transform
IPL	Image Processing Laboratory
JPL	Jet Propulsion Laboratory
LACMA	Los Angeles County Museum of Art
VICAR	Video Image Communication and Retrieval

## CONTENTS

1.	INTRODUCTION . . . . .	1-1
2.	SIMULATION EXPERIMENT . . . . .	2-1
3.	IMAGE-PROCESSING ANALYSIS . . . . .	3-1
4.	CONCLUSION . . . . .	4-1
	REFERENCES . . . . .	5-1

### Figures

1.	Enhanced Images of Scanned Negatives	
(a)	Sheet A - Control - Before (3/30/82) - PDS Scan CDF Stretch . . . . .	3-3
(b)	Sheet A - Control - After (8/31/82) . . . . .	3-4
(c)	Sheet B - Experimental - Before (3/30/82) . . . . .	3-5
(d)	Sheet B - Experimental - Intermediate #1 (5/6/82) . . . . .	3-6
(e)	Sheet B - Experimental - Intermediate #2 (6/10/82) . . . . .	3-7
(f)	Sheet B - Experimental - After (8/31/82) . . . . .	3-8
(g)	Sheet C - Experimental - Before (3/30/82) . . . . .	3-9
(h)	Sheet C - Experimental - After (8/31/82) . . . . .	3-10
2.	Registered Subareas for Sheet B, Area 1	
(a)	Subarea 1 - Before (3/30/82) - Registered - Apodized . . . . .	3-12
(b)	Subarea 1 - Intermediate #1 (5/6/82) . . . . .	3-13
(c)	Subarea 1 - Intermediate #2 (6/10/82) . . . . .	3-14
(d)	Subarea 1 - After (8/31/82) . . . . .	3-15
3.	One-Dimensional Fast Fourier Transforms (FFTs) of Sheet A	3-17
4.	One-Dimensional FFTs of Sheet B	
(a)	Area 1 . . . . .	3-18
(b)	Area 2 . . . . .	3-19

5. One-Dimensional FFTs of Sheet C . . . . .	3-20
6. Enhanced Difference Image of Sheet A Registered Subarea .	3-21
7. Enhanced Difference Image of Sheet B, Subarea 1	
(a) Before - Intermediate #1 . . . . .	3-23
(b) Before - Intermediate #2 . . . . .	3-24
8. Enhanced Difference Image of Sheet B, Subarea 2	
(a) Before - Intermediate #1 . . . . .	3-25
(b) Before - Intermediate #2 . . . . .	3-26
9. Enhanced Difference Image of Sheet C, Before - After . . .	3-28

#### Tables

1. JPL Photolab Numbers for Figures . . . . .	4-2
---	-----

## 1.0 Introduction

Early in the sixteenth century, Leonardo da Vinci wrote a set of illustrated notes on a variety of subjects which includes astronomy, hydrodynamics, light and the earth sciences (Armand Hammer Foundation, 1981). The concepts of steam power and the submarine appear for the first time in these notes. Leonardo wrote from right to left, possibly in an attempt to obscure the nature of his work. The notes consist of 18 sheets of paper, folded in half, containing writing and diagrams on the front and rear, so that each sheet consists of four working pages, for a total of 72 pages.

In the seventeenth century, the notes were bound in leather. In the eighteenth century the manuscript was given the title "Of the Nature, Weight and Movement of Water", and was sold to the Earl of Leicester. It remained in his family until its purchase at Christie's in London in December 1980 by Dr. Armand Hammer. It is now known as the Codex Hammer.

Dr. Hammer wished to have the sheets mounted so that they could be exhibited to expose both sides to the viewer. Victoria Blyth-Hill of the Los Angeles County Museum of Art returned the Codex Hammer to its original state by removing the manuscript from its binding. The unbound sheets were examined for condition and prepared for mounting, in a type of mount developed by Michael Warnes at Windsor Castle. The mount consists of two very thin layers of plexiglas, sealed around the edges, with each sheet of paper held in place by silk tabs.

The long-term effects of the plexiglas encapsulation technique were not completely researched prior to the mounting of the Codex Hammer. Because the sheets are made of handmade paper, which is hygroscopic and dimensionally unstable, they are constantly moving. The direct contact with the plexiglas might lead to a "micro-burnishing" effect which could potentially degrade the surface texture of the Codex. Because the sheets are completely sealed in the plexiglas, they may be subject to stresses caused by the micro-climate inside the plexiglas responding to changes in the outside temperature and humidity.

The purpose of the research reported here was to assist the Los Angeles County Museum of Art in determining if there is potential long-term danger to the Codex Hammer as a result of the mounting technique. The information developed should have application to manuscripts in general.

## 2.0 SIMULATION EXPERIMENT

James Druzik of the Los Angeles County Museum of Art (LACMA) chose three sheets of seventeenth century handmade paper with which to simulate the Codex. One sheet, "A", was set aside as a control. Two sheets, "B" and "C", were the experimental samples. A raking-light photographic facility was implemented at LACMA. It consisted of an electrostatic plate rigidly attached to a wall, a rigidly attached light source positioned at a two-degree angle with respect to the plane of the electrostatic plate, and a 35-millimeter camera. This section of the laboratory was sealed off so that the apparatus could not be accidentally bumped. The electrostatic plate was used to hold each sheet flat, in a repeatable position, without creating undue force. The light source was used to provide repeatable raking-light illumination in order to highlight the surface texture and deformations of the sheets.

All three sheets were photographed under raking light by LACMA personnel and encapsulated in plexiglas in the same manner as the Codex Hammer. The two test sheets were subjected to daily extremes of temperature, humidity and lighting in a LACMA environmental test chamber. The temperature excursions ranged from 70° to 110° and the humidity from 30% to 70% RH. All three sheets were photographed before, at intermediate stages of, and after a total of five months of environmental cycling. A number of exposure-bracketed negatives were supplied to the Jet Propulsion Laboratory (JPL) for analysis. It should be noted that JPL performed no analysis of and bears no responsibility for the consistency of the geometry of the raking-light photography or of the applicability of the simulation to the actual Codex Hammer.



### 3.0 IMAGE PROCESSING ANALYSIS

Analysis of the negatives supplied to JPL was performed at the Image Processing Laboratory (IPL). The IPL was established about twenty years ago to support NASA's unmanned exploration of the moon and the planets. Images from the Ranger and Surveyor missions to the moon, the Mariner missions to Mercury, Venus, and Mars, the Viking landing on Mars, and the Voyager flybys of Jupiter and Saturn were processed in the IPL. A separate Biomedical IPL was established and is currently studying cancer, arteriosclerosis, and other diseases. The work of the IPL has diversified in recent years to include earth resources, geology applications, military projects, art conservation, and other areas.

Eight of the supplied negatives of the Codex Hammer mockup were chosen for analysis. They are sheet A on 3/30/82 ("before") and 8/31/82 ("after"), sheet C on the same dates and sheet B on the same dates plus two intermediate dates (5/6/82; 6/10/82).

The negatives were "scanned" and converted to computer-readable data with the IPL's PDS microdensitometer. This device consists of a movable glass computer-controlled stage and a light source and associated optics which direct a narrow, adjustable beam of light through the glass stage. A light sensor and associated optics sense the amount of light passing through the stage from the source. The above elements reside on a massive, dimensionally stable granite platform. The operation and data collection are controlled by a minicomputer in an adjacent room.

The system is operated by placing each negative securely on the glass stage and aligning it. The amount of light passing through the negative is detected and converted to a number from 0 to 255. Zero represents black, 255 represents white, and intermediate numbers represent various shades of grey called the "grey level" or DN (digital number). This number is sensed for a rectilinear array of points on the negative. Each point is known as a pixel (short for "picture element"). Limitations of project resources dictated a

maximum number of pixels of 1000 lines by 1500 samples, or 1.5 million total pixels per negative. Considerations of resolution of small features ("wire lines") in the simulation sheets led to a choice to scan with a  $20\mu$  (micron) light spot size and  $10\mu$  pixel spacing on the negative. This limited the area of each negative that could be scanned to approximately one-fourth of the total area. These areas were chosen, for each sheet, to avoid the regions of large cockles insofar as possible. The cockles are large deformations or "hills" in the sheets, which under raking light are saturated completely white or black, i.e. they fall outside the dynamic range of the film. It is desirable to avoid such regions in the analysis.

The eight negatives were scanned and the resulting magnetic tape converted to a form compatible with the IPL's VICAR (Video Image Communication and Retrieval) computer language. The IPL consists of an IBM 370/158 mainframe computer, associated tape drives, disc drives, etc., and an array processor. A PDP-11/40 minicomputer communicates between the IBM and the interactive image processing hardware, i.e., Ramtek and Comtal image and graphics display devices which control a variety of black-and-white and color monitors. Also in the IPL is a series of playback devices for converting a processed image from computer tape into negatives and prints, a video disc system, a coordinate digitizer, a plotter, a Dunn camera for producing up to 8 x 10 inch color Polaroids, and other associated hardware.

The contrast of each of the eight images was adjusted with a "ramp cumulative distribution function" (ramp CDF) contrast stretch in such a way that the distribution of grey levels in each image was very nearly equal. The results are shown in Figure 1 (a-h). These prints were made by converting the processed images on computer tape back into negatives on a Dicomed playback device. The eight images in Figure 1 all show the cockles (large hills), the wire lines (closely spaced linear periodic structures), and deformations of intermediate size ("mesoscale deformations"). The water mark on sheet B appears distinctly. As an indication of scale, the separation between the top two registration marks (crosses) on sheet B is 14.3 cm.

ORIGINAL PAGE IS  
OF POOR QUALITY

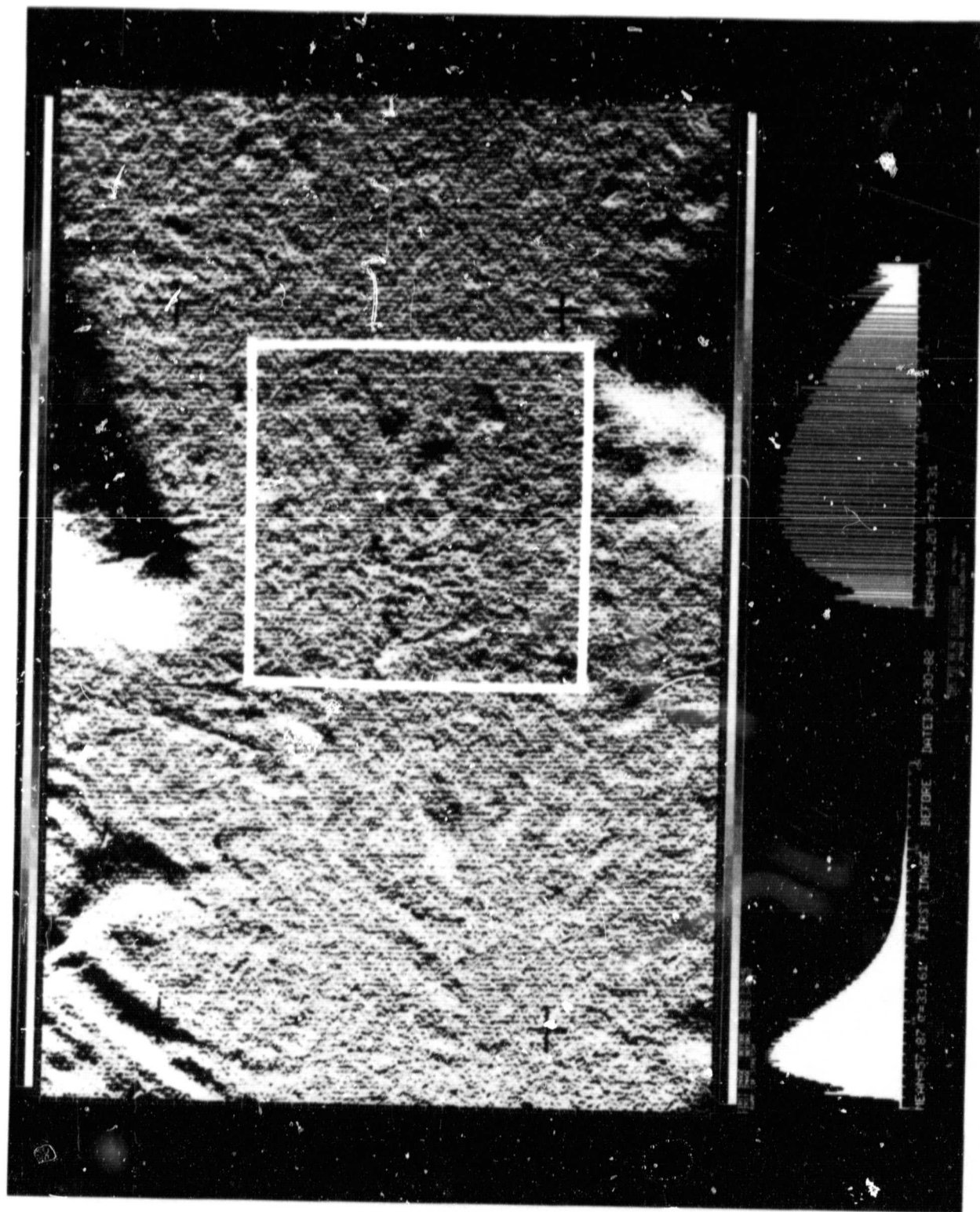


Figure 1a. Sheet A - Control - Before (3/30/82) - PDS Scan - CDF Stretch

ORIGINAL PAGE IS  
OF POOR QUALITY

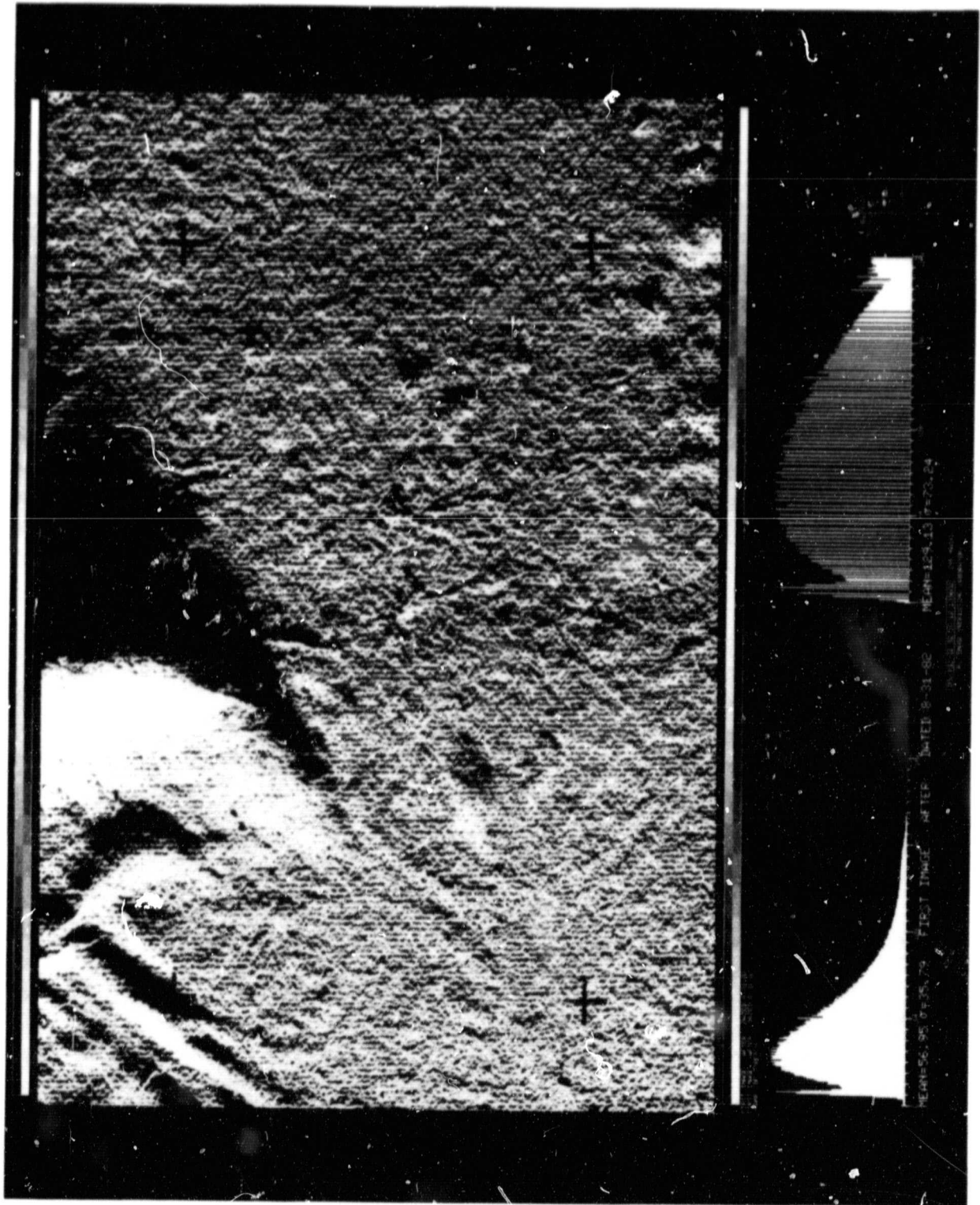


Figure 1b. Sheet A - Control - After (8/31/82)

ORIGINAL PAGE IS  
OF POOR QUALITY

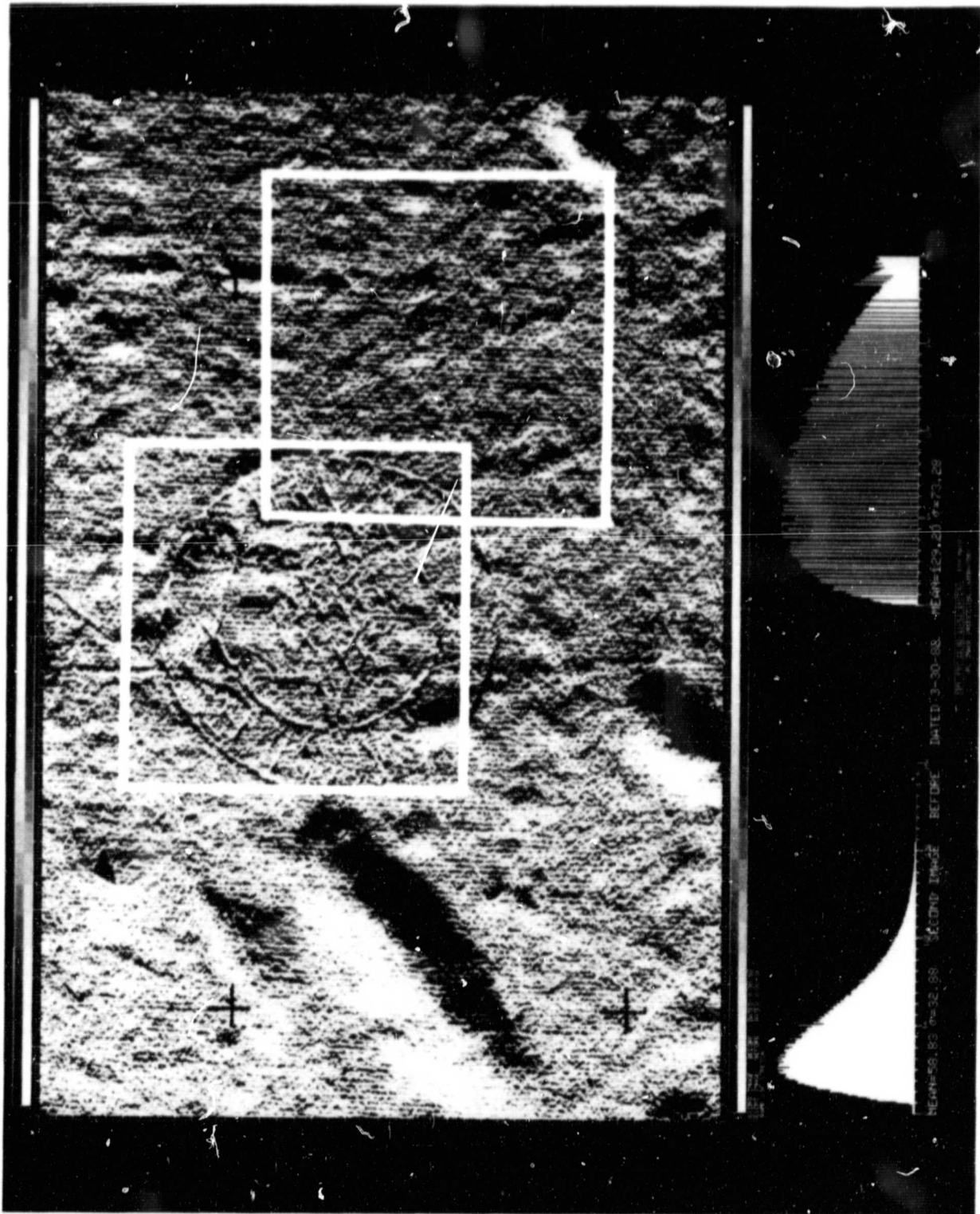


Figure 1c. Sheet 3 - Experimental - Before (3/30/82)



ORIGINAL PAGE IS  
OF POOR QUALITY

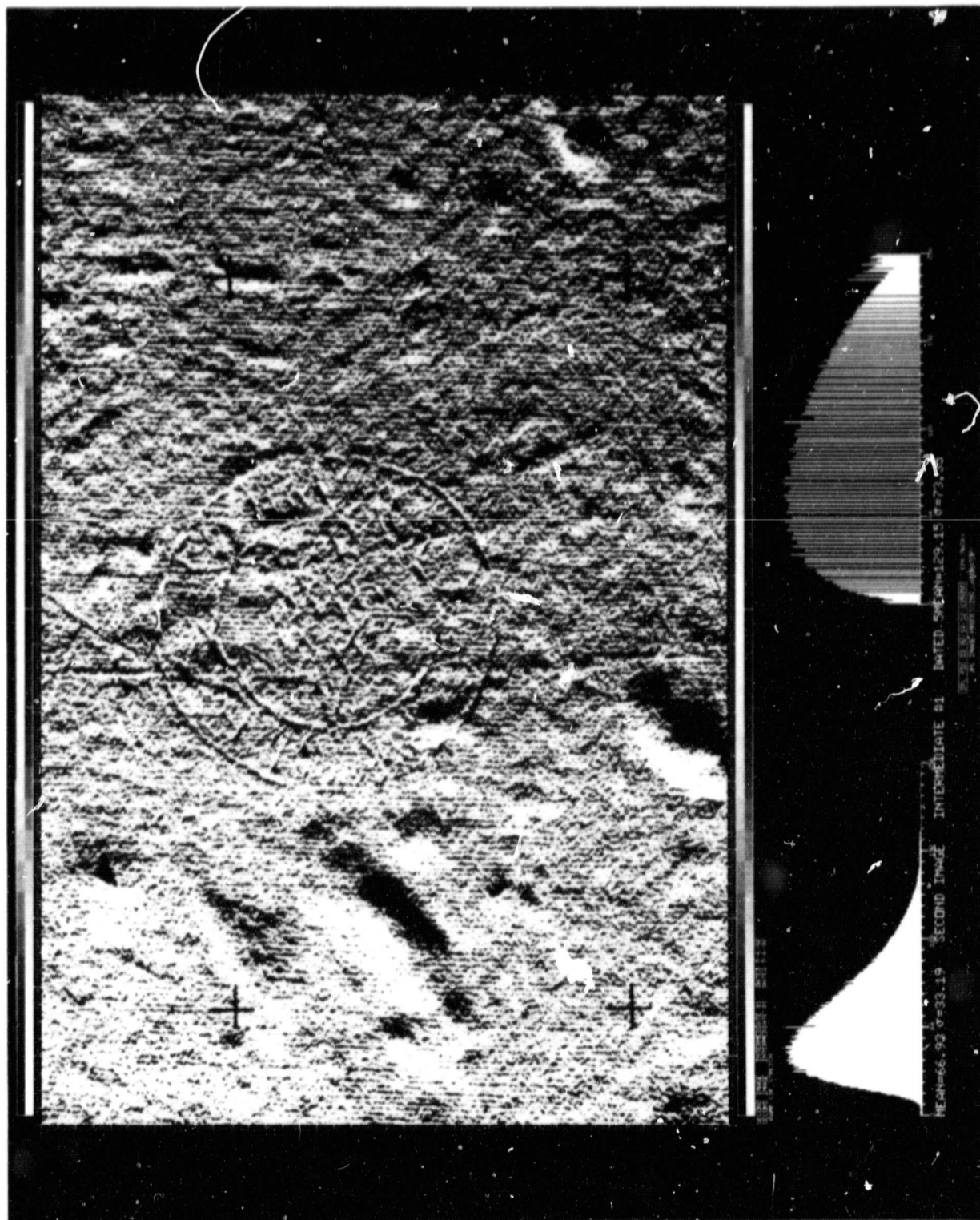


Figure 1d. Sheet B - Experimental! - Intermediate #1 (5/6/82)

ORIGINAL PAGE IS  
OF POOR QUALITY

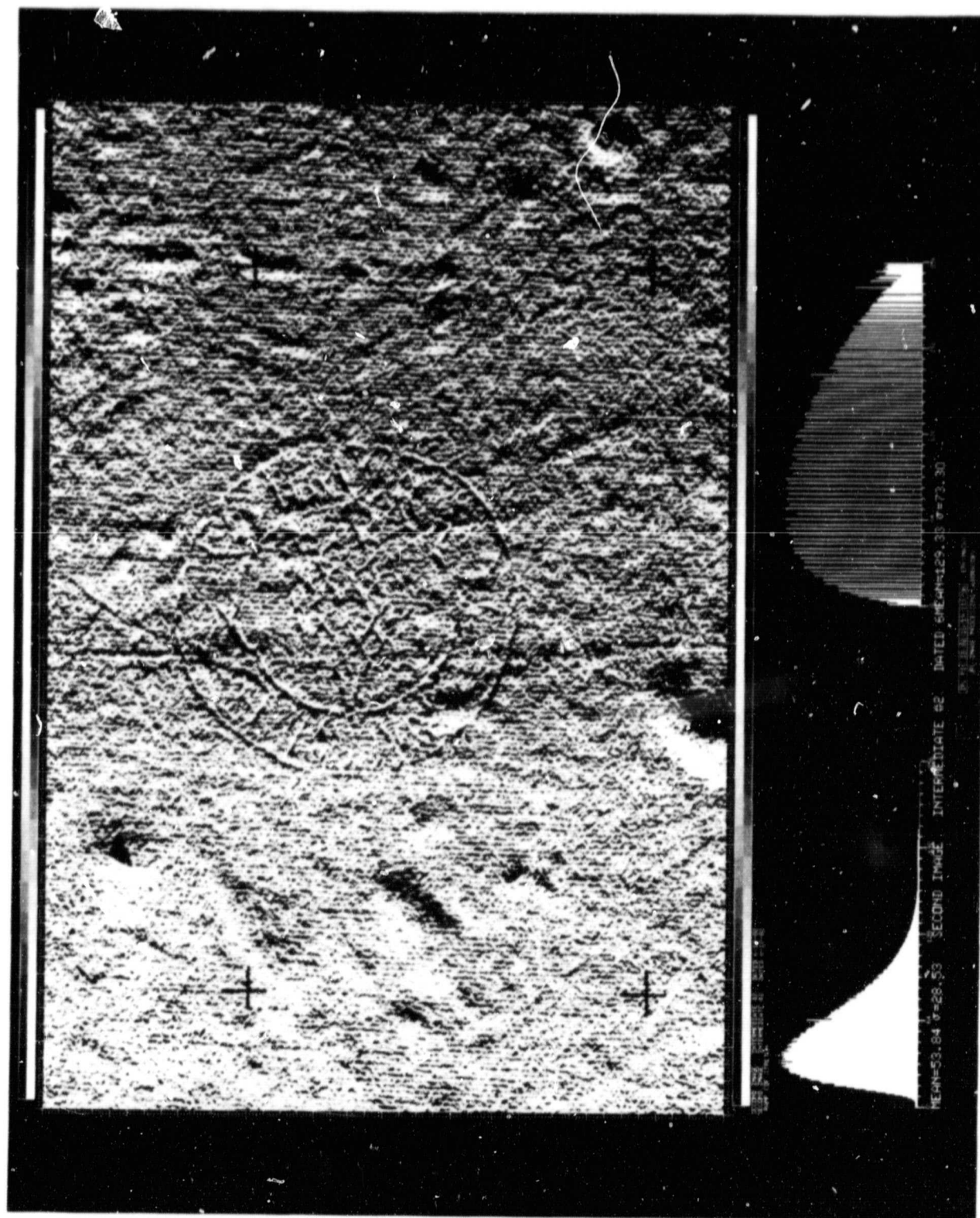


Figure 1e. Sheet B - Experimental - Intermediate #2 (6/10/82)

ORIGINAL PAGE IS  
OF POOR QUALITY

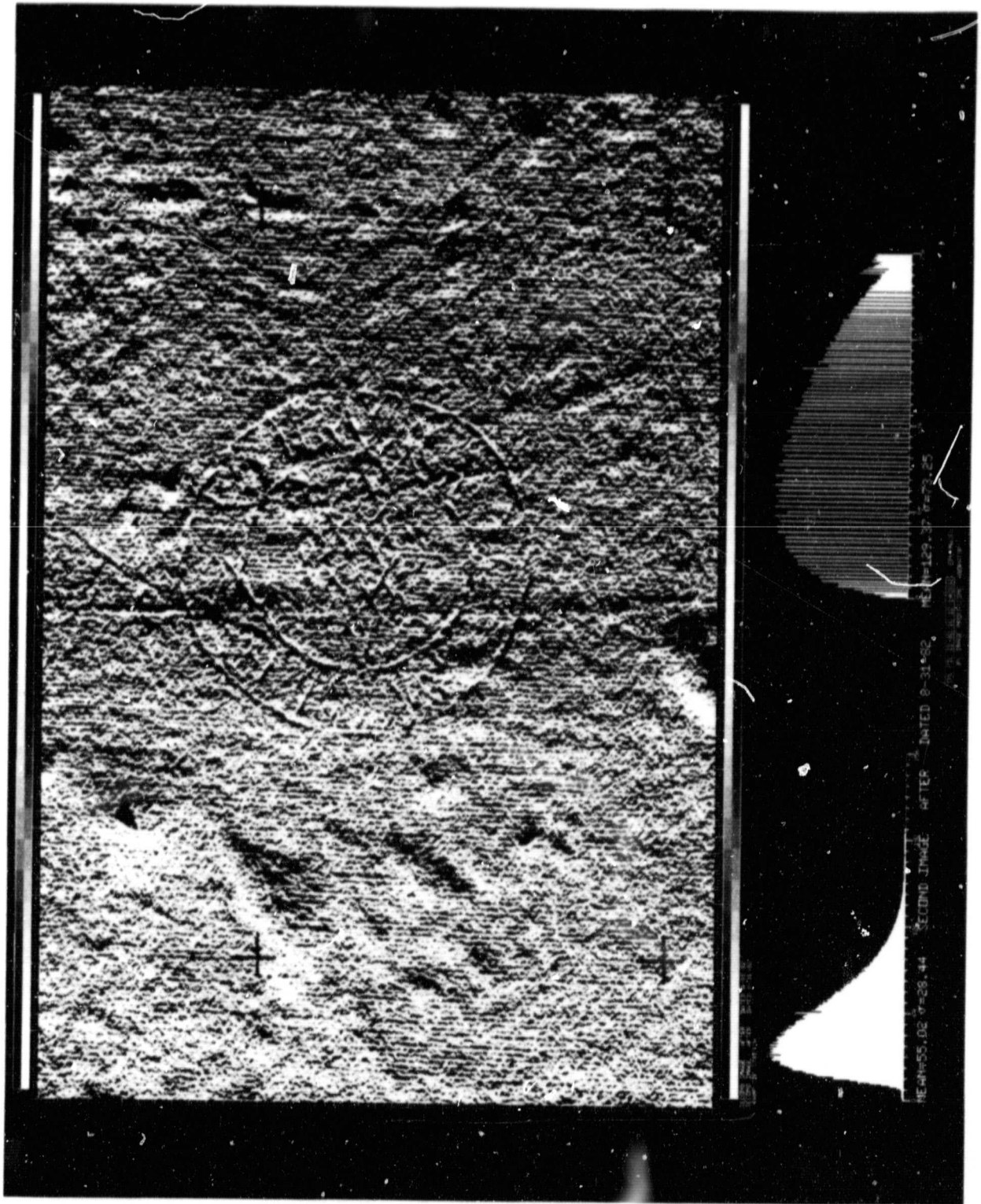


Figure 1f. Sheet B - Experimental - After (8/31/32)



ORIGINAL PAGE IS  
OF POOR QUALITY

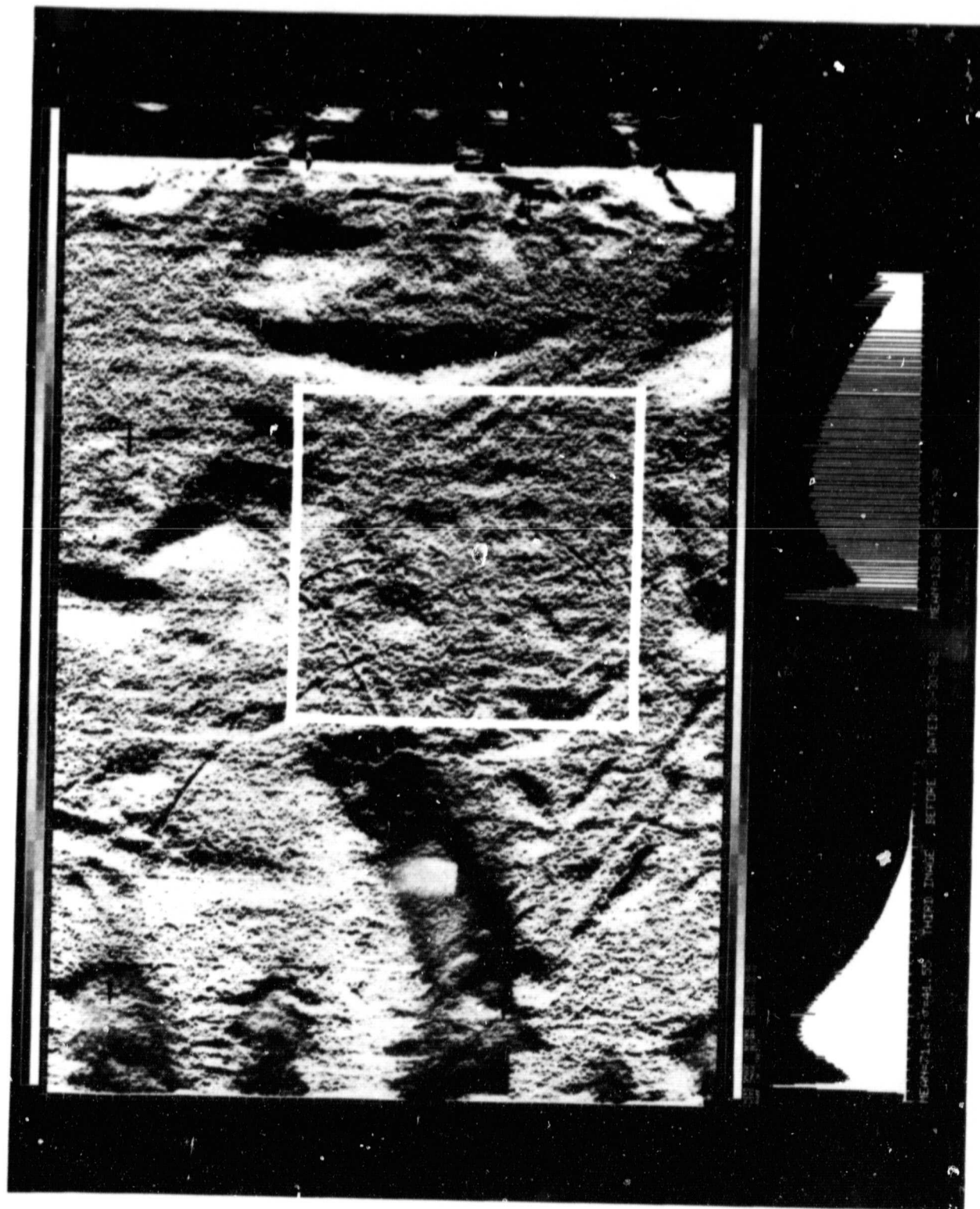


Figure 1g. Sheet C - Experimental - Before (3/30/82)

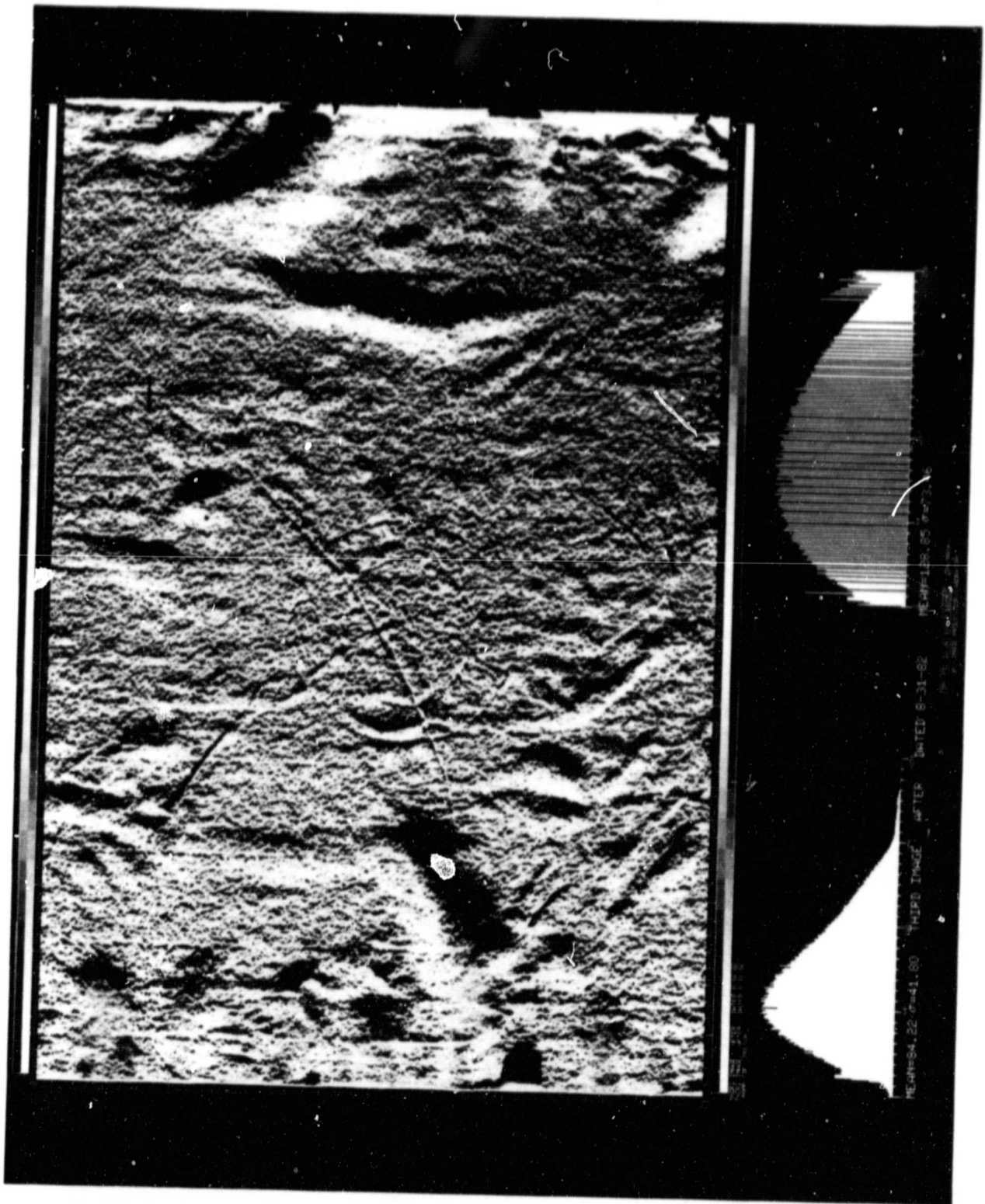


Figure 1h. Sheet C - Experimental - After (8/31/82)

The printed scales along the picture border measure the number of vertical lines (1000) and the number of horizontal samples (1500) in the images. The IPL processing history is given at the bottom of each image. Also shown are the image histograms before and after the ramp CDF stretch was applied. These histograms display the distribution of grey levels in an image. They are plots of grey level on the X-axis vs. the number of pixels with a given grey level on the y-axis. The ramp CDF stretch has "stretched out" the raw histograms (left) to yield the processed histograms (right).

Next, for each sheet (A, B, C) the images of that sheet were geometrically registered or aligned with respect to one another to ensure that precisely the same area of each sheet would be analyzed. This was done using registration marks that had previously been drawn on the sheets for this purpose. Then, owing to size restrictions in the next processing step, subareas of each image in Figure 1 were chosen for detailed analysis. The areas are 512 x 512 pixels in size and are indicated in Figure 1a, c and g. Two different areas were chosen from sheet B, the most promising experimental sheet. All subareas were chosen to completely avoid the cookies.

One of the sheet B subareas is shown in Figure 2 (a-d). The striped area around the image border is a result of the process of "apodizing" the data. This treatment has minimal effect on the image and prevents the introduction of spurious data into the next step of the processing.

A one-dimensional Fast Fourier Transform (FFT) analysis was performed on the twelve image subareas. The FFT is a numerical technique used to analyze the spatially or temporally varying characteristics of signals. It works essentially by fitting an infinite series of sine waves of different frequency and amplitude to a signal. It gives a measure of the relative amounts of components of different frequencies that are contained in a signal. The signal can be either space-varying, as are the images in this study, or time-varying, as is the music coming from a speaker. Thus we may speak of spatial frequency or temporal frequency.

ORIGINAL PAGE IS  
OF POOR QUALITY

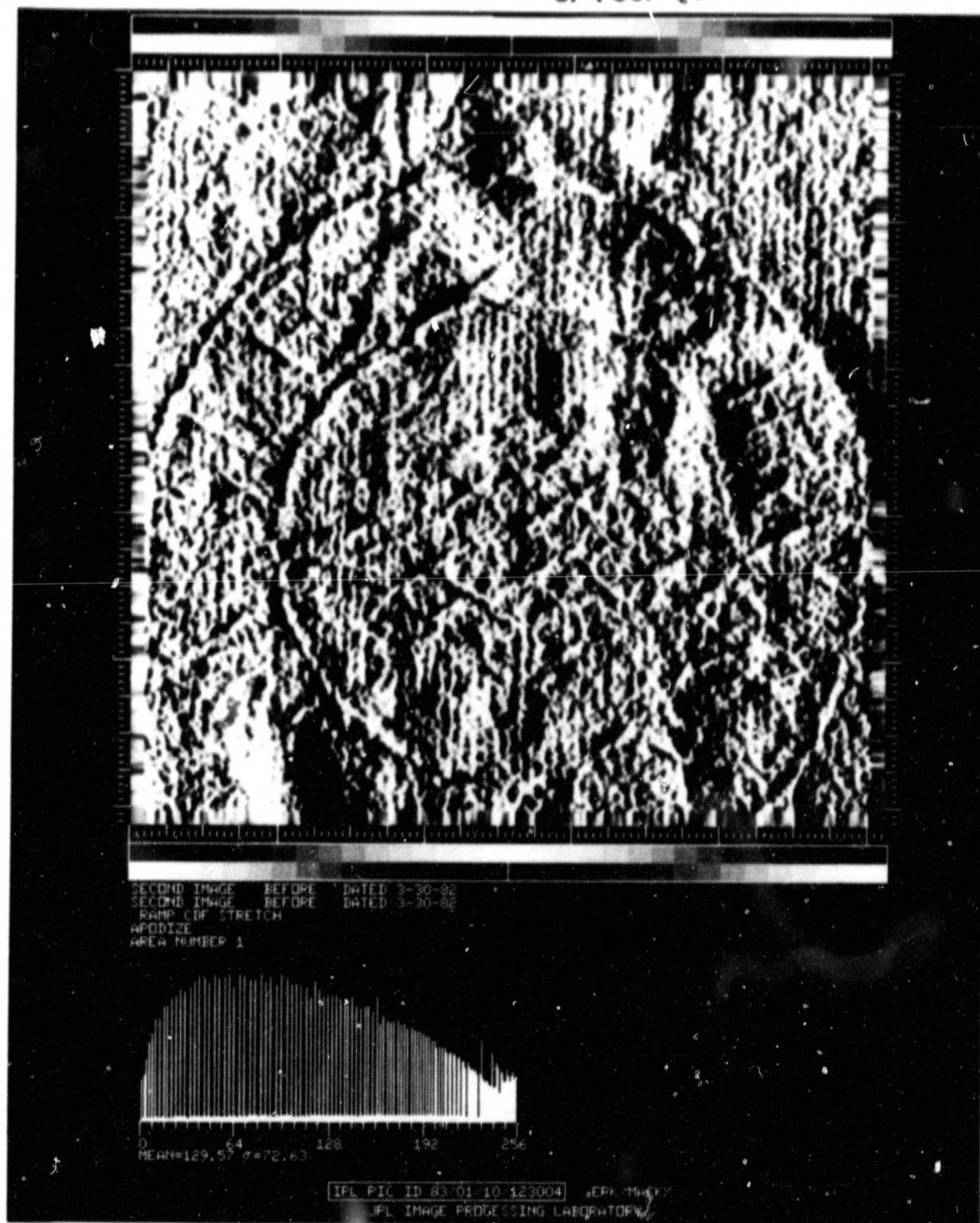


Figure 2a. Subarea 1 - Before (3/30/82) - Registered - Apodized



ORIGINAL PAGE IS  
OF POOR QUALITY

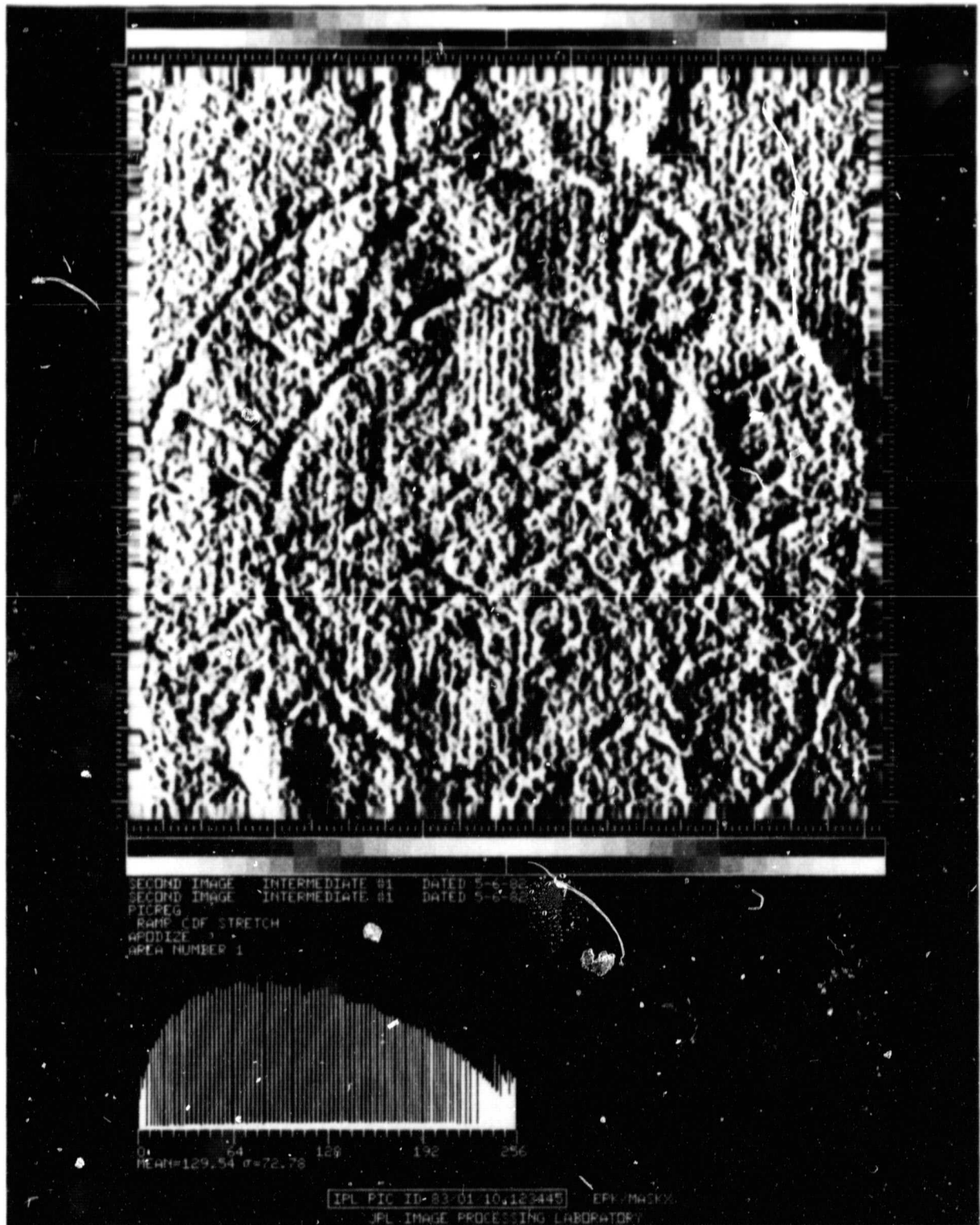


Figure 2b. Sheet B - Subarea 1 - Intermediate #1 (5/6/82)

ORIGINAL PAGE IS  
OF POOR QUALITY

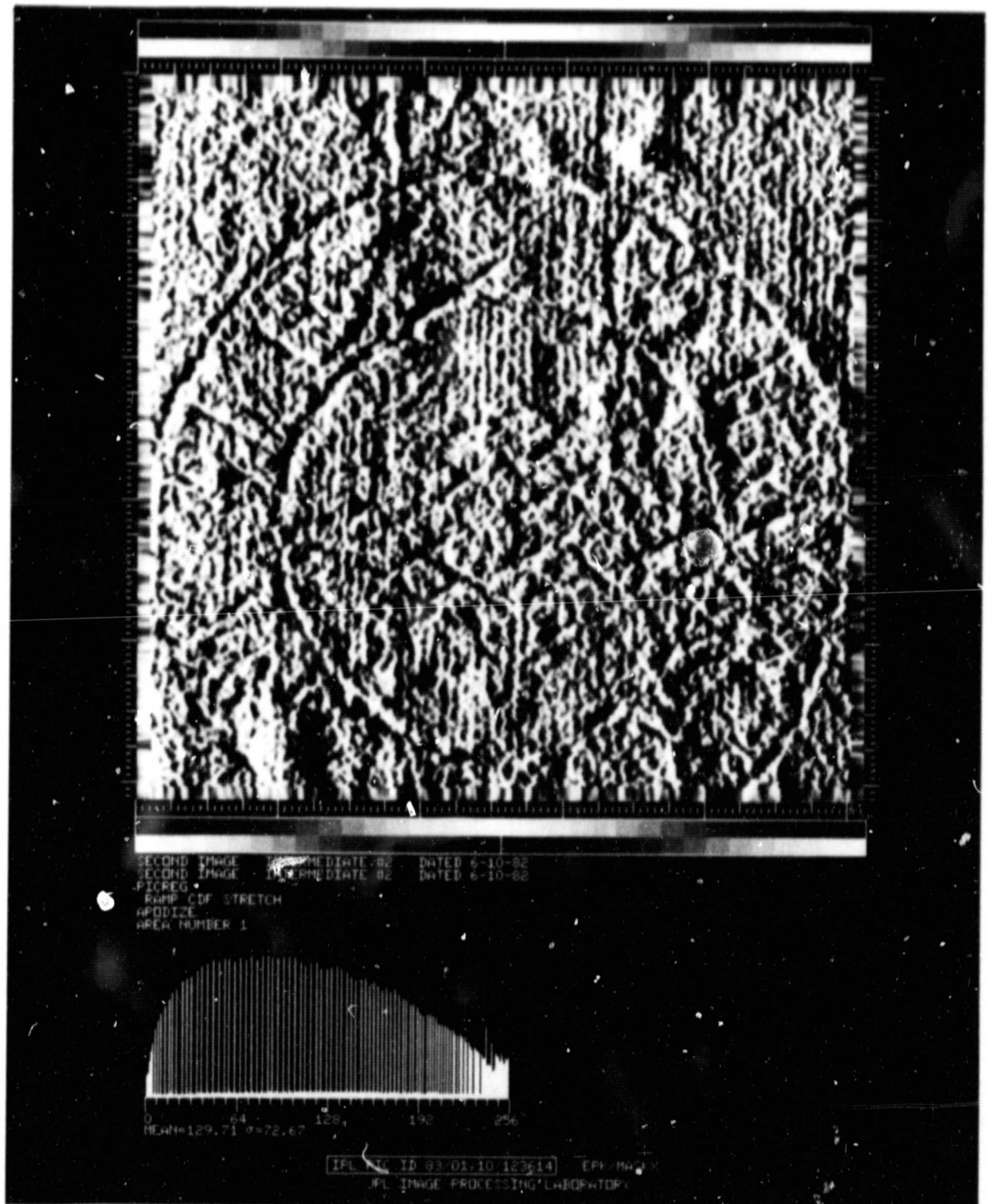


Figure 2c. Sheet B - Subarea 1 - Intermediate #2 (6/10/82)

ORIGINAL PAGE IS  
OF POOR QUALITY



Figure 2d. Sheet B - Subarea 1 - After (8/31/82)

Initially, one-dimensional and two-dimensional FFT's were analyzed, hence the necessity for limiting the subareas to 512 pixels in both directions. The 1-D FFT analysis was found to be more suited to this task. In the 1-D process, the FFT is computed separately for each line of the image. The separate FFTs are averaged and displayed as a line plot.

Figure 3 shows the before and after FFTs for sheet A (the control). The x-axis of this plot, originally spatial frequency, has been converted to spatial size in pixels. The numbers on the y-axis are a measure of the logarithm of the amplitude of the FFT, which tells which sizes predominate. Of most significance are any peaks which stand out relative to the points in their immediate vicinity. For instance, the large peak at 8 pixels corresponds to the wire lines. There is no significant variation between the two plots, i.e., no degradation can be detected for the control sheet. Figures 4a and 4b show all four FFTs for sheet B, subareas 1 and 2, respectively. Note how the wire line peak does not change, which indicates that these features are not degrading. However, for certain spatial frequencies there is significant, consistent degradation over time. This degradation is limited to the broad peak spanning the range from approximately 50 to 120 pixels, with a median scale of about 70 pixels. The conversion from pixels to millimeters on the sheets themselves is 7.5 pixels/mm. The features that are degrading are the "mesoscale" deformations with typical sizes of 7 mm and typical spacings of 9 mm. These are the largest deformations visible in the apodized subframes. These are the only significant variations in the FFTs and, according to our understanding, represent no degradations of concern to LACMA. (Note interestingly that no degradation is seen for the period 6/10-8/31/82.)

As expected, the results for sheet C are inconclusive (Figure 5). The original images are poor, and cockling is widespread.

Figure 6 is an enhanced difference image of the subarea for sheet A. It was made by subtracting the 8/31/82 registered subarea from the 3/30/82 registered subarea and contrast enhancing the result. The neutral grey character of the image indicates a lack of degradation or of differential stretching of the



ORIGINAL PAGE IS  
OF POOR QUALITY

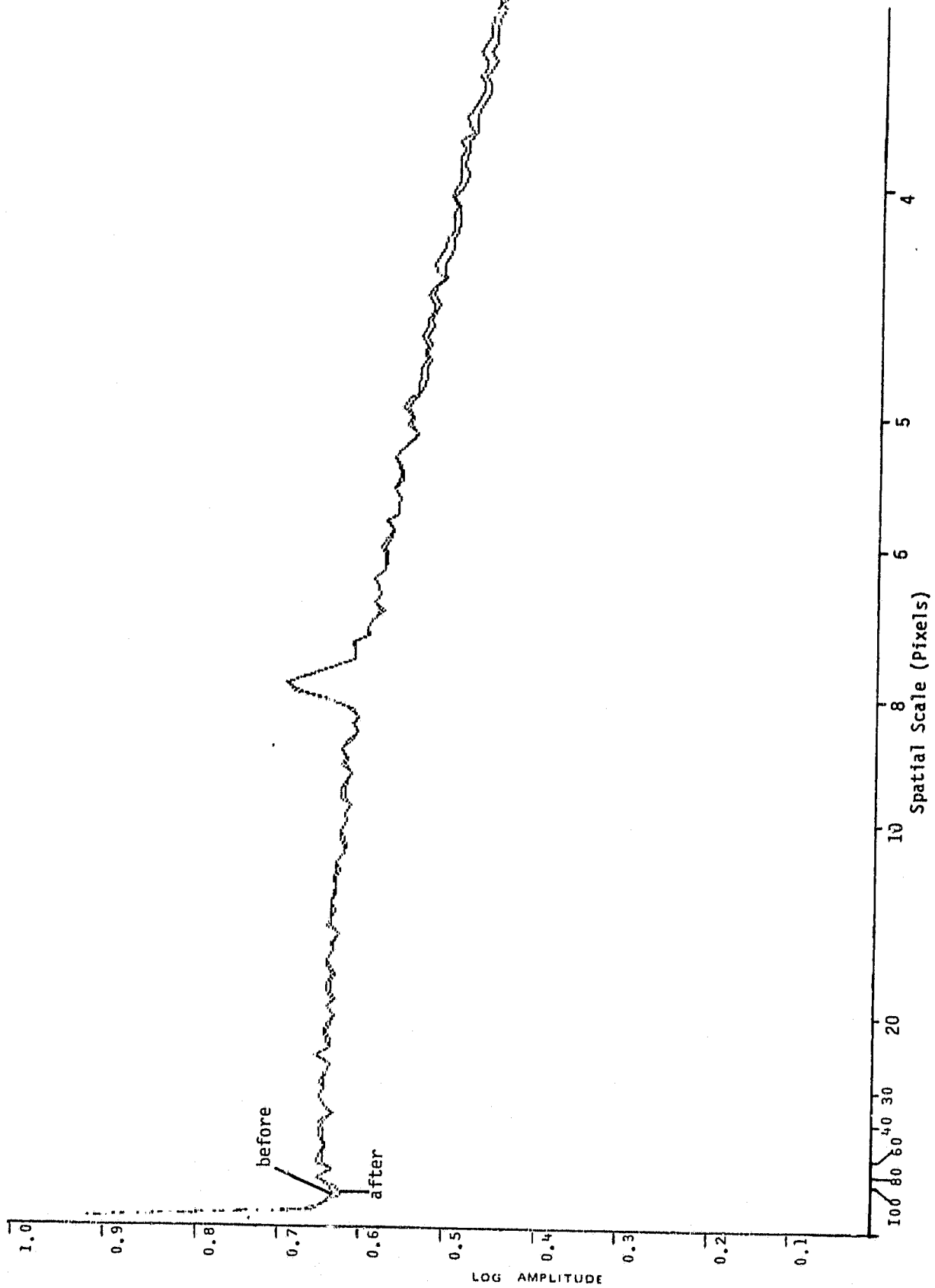


Figure 3. One-Dimensional Fast Fourier Transforms (FFTs) of Sheet A

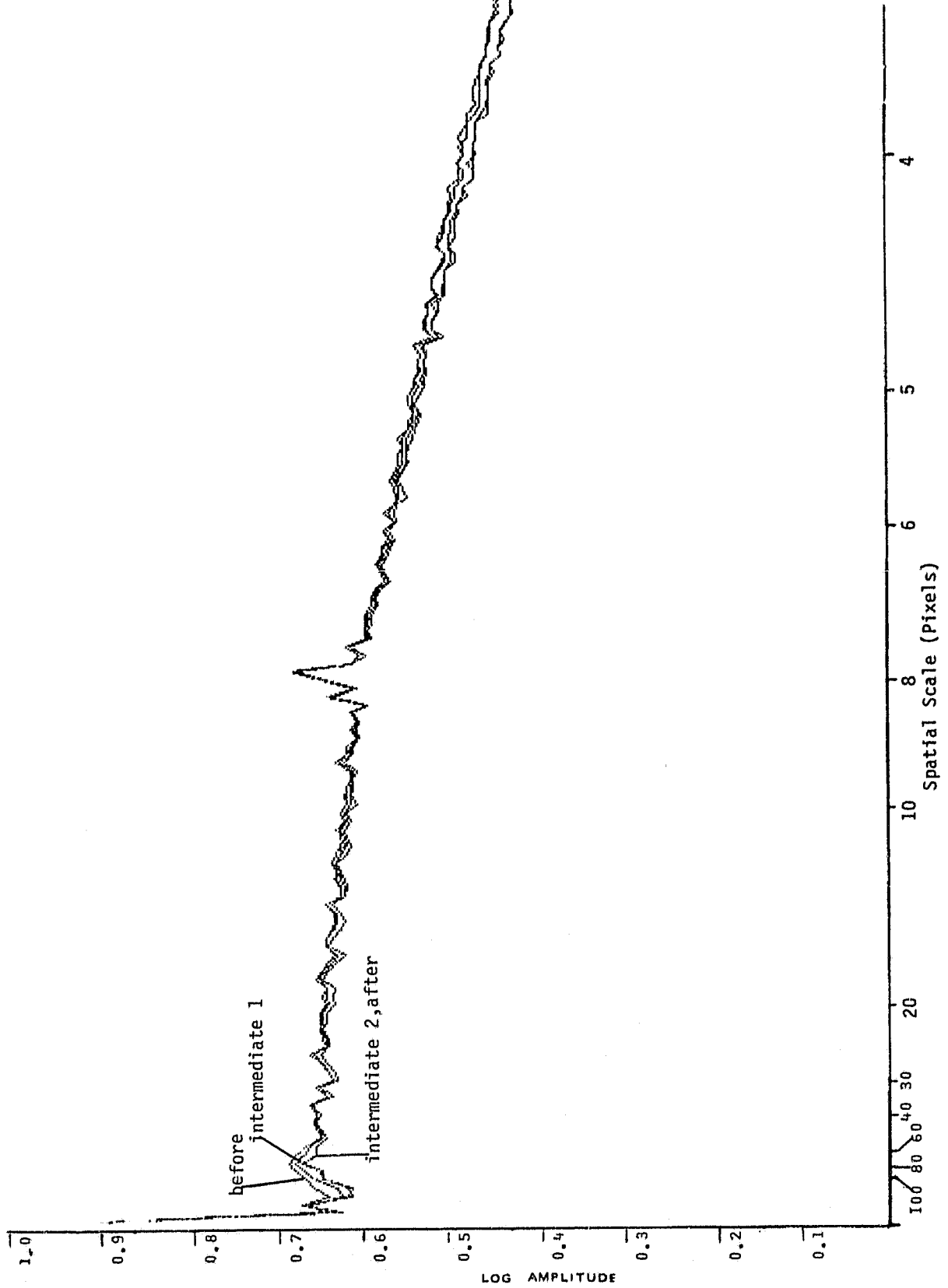


Figure 4a. One-Dimensional Fast Fourier Transforms (FFTs) of Sheet B, Area 1

ORIGINAL PAGE 10  
OF POOR QUALITY

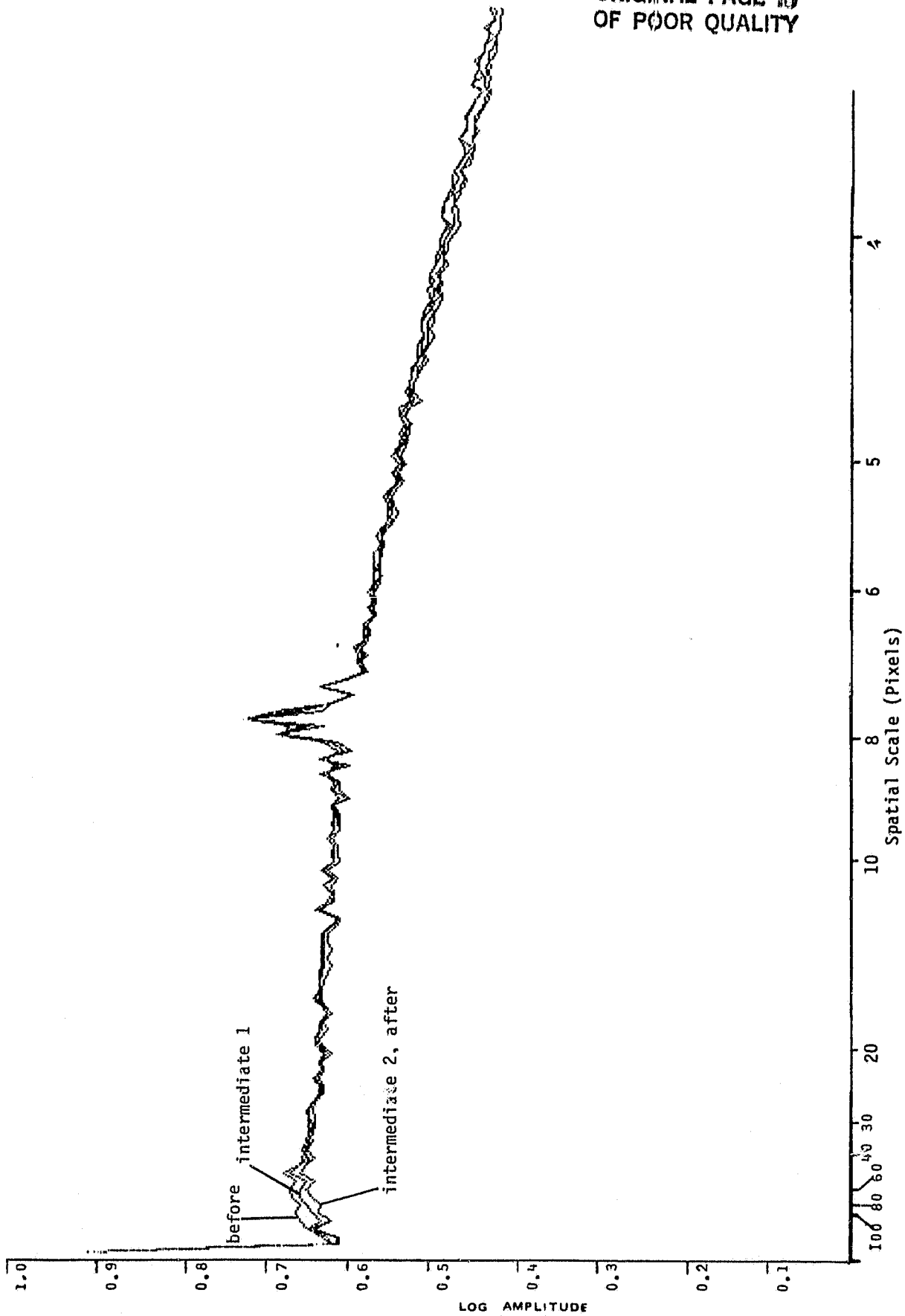


Figure 4b. One-Dimensional Fast Fourier Transforms (FFTs) of Sheet B, Area 2

ORIGINAL PAGE 19  
OF POOR QUALITY

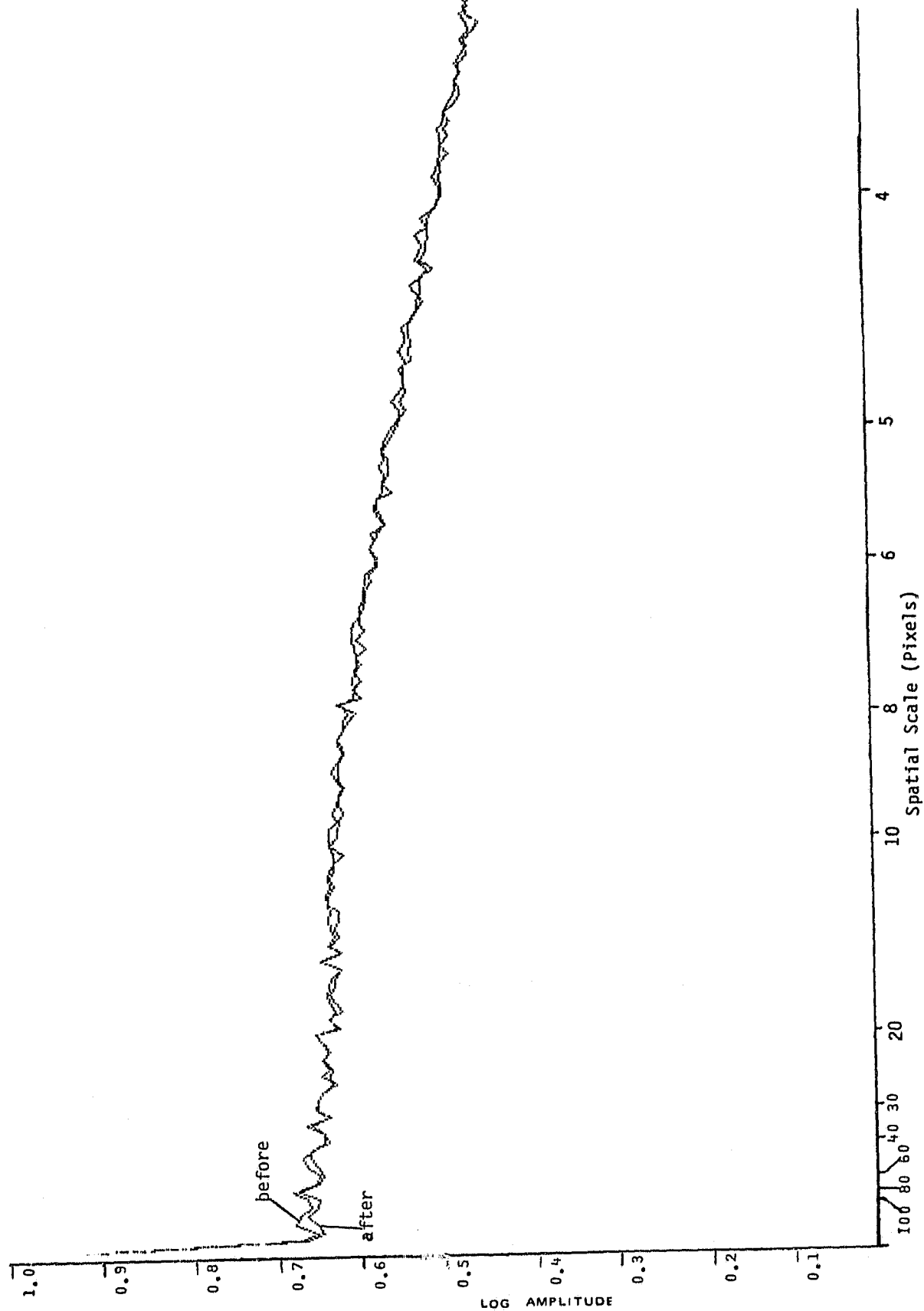


Figure 5. One-Dimensional Fast Fourier Transforms (FFTs) of Sheet C

ORIGINAL PAGE IS  
OF POOR QUALITY

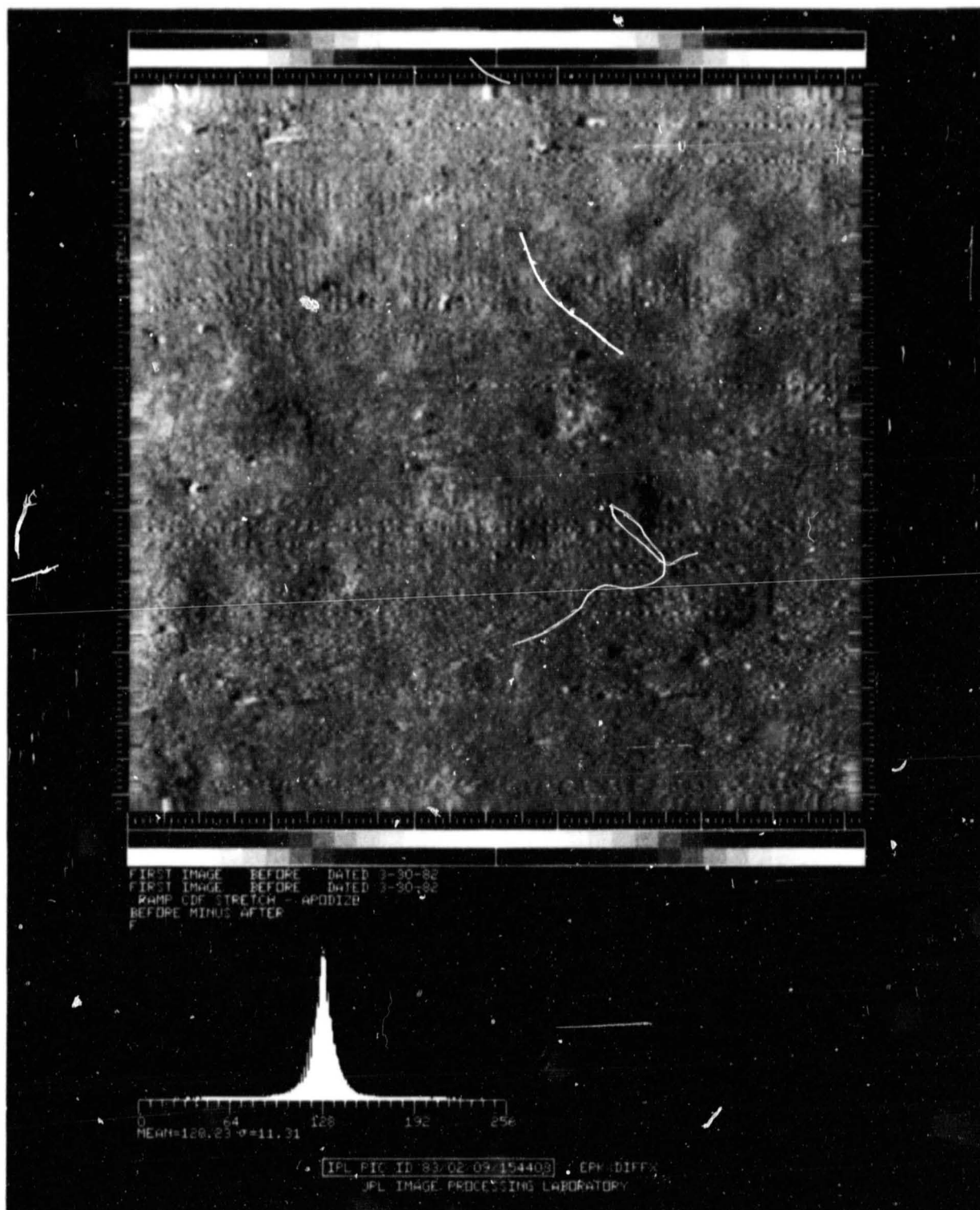


Figure 6. Enhanced Difference Image of Sheet A Registered Subarea

control sheet during the period of the experiment. Figures 7a-b are similar difference images for area 1 of sheet B. In Figure 7a, the registered subarea on 5/6/82 was subtracted from that on 3/30/82. In Figure 7b, the 6/10/82 image was subtracted from that on 3/30/82. The difference image for 8/31/82 is similar to 7b.

These images show the locations of the mesoscale deformations that the FFTs indicate are degrading, i.e., are becoming less pronounced over time. They appear as large (50-100 pixels in these 512 x 512-pixel images) black-and-white dimples in Figure 7. With hindsight, one can go back to the series of images in Figure 2 and see the amplitudes of these deformations changing.

Unlike the control sheet, the difference images of sheet B exhibit fine-scale detail which increases with time during the experiment. This is caused by slight shifts in the location of the wire lines with time. Because their edges are in slightly different locations in the two images, the wire lines appear as a strong signal in the difference images.

Is this indicative of stretching of sheet B, or simply of misregistration of the images in the computer? Figure 6, the difference image of sheet A, suggests that the registration is excellent because the wire line signal does not appear. Another demonstration that registration is not the problem is given in Figures 8 a-b, the difference images for area 2 of sheet B. Referring back to Figure 1c, we see that area 1 is far from the geometrical registration marks, while area 2 is between two of the marks. The computer registration is performed by locating these marks in both frames to be registered and forcing their positions in one image to match those in the other image, then linearly interpolating in between. The fact that the wire line signal vanishes in Figure 8 in the area between the two registration marks and appears neutral grey, like Figure 6, indicates that the registration is excellent. The fact that the wire line signal appears elsewhere in Figure 8 and everywhere in Figure 7 indicates that differential stretching of sheet B is occurring. (The fact that the wire line signal increases with time also indicates that the sheet is stretching. Misregistration would be random,

ORIGINAL PAGE IS  
OF POOR QUALITY

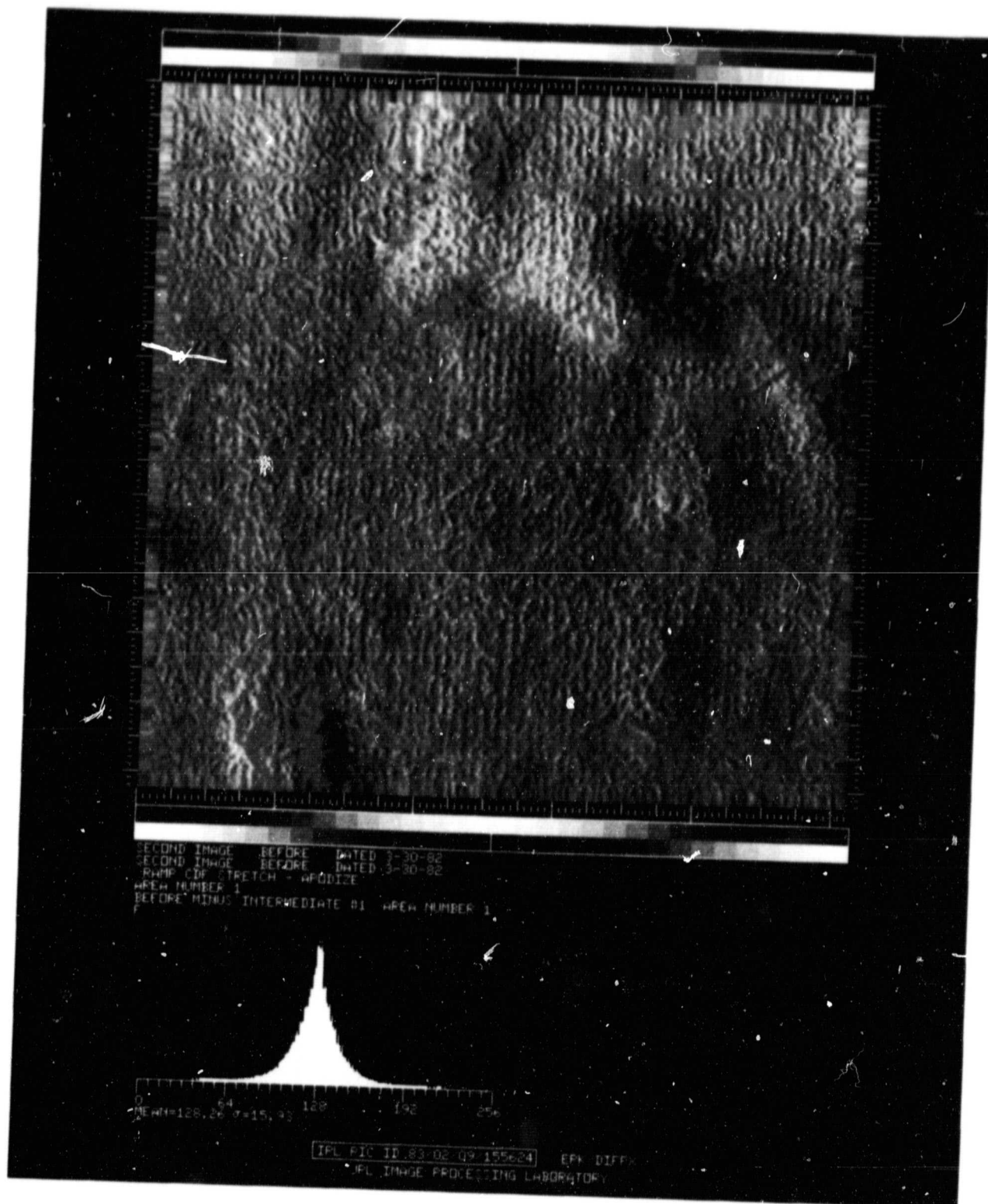


Figure 7a. Enhanced Difference Image of Sheet B Subarea 1, Before-Intermediate #1

ORIGINAL PAGE IS  
OF POOR QUALITY



Figure 7b. Enhanced Difference Image of Sheet B Subarea 1, Before-Intermediate #2



ORIGINAL PAGE IS  
OF POOR QUALITY

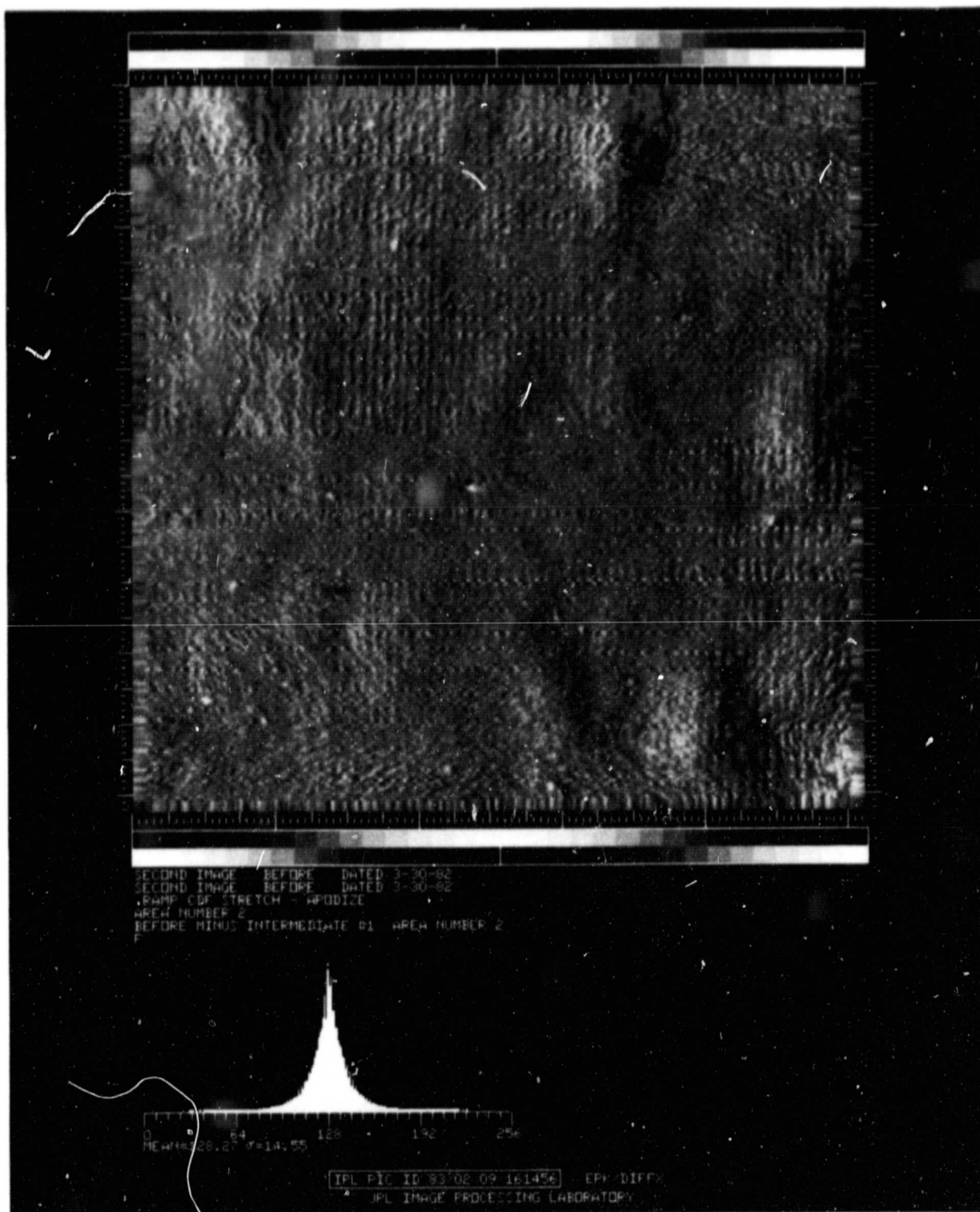


Figure 8a. Enhanced Difference Image of Sheet B Subarea 2, Before-Intermediate #1

ORIGINAL PAGE IS  
OF POOR QUALITY

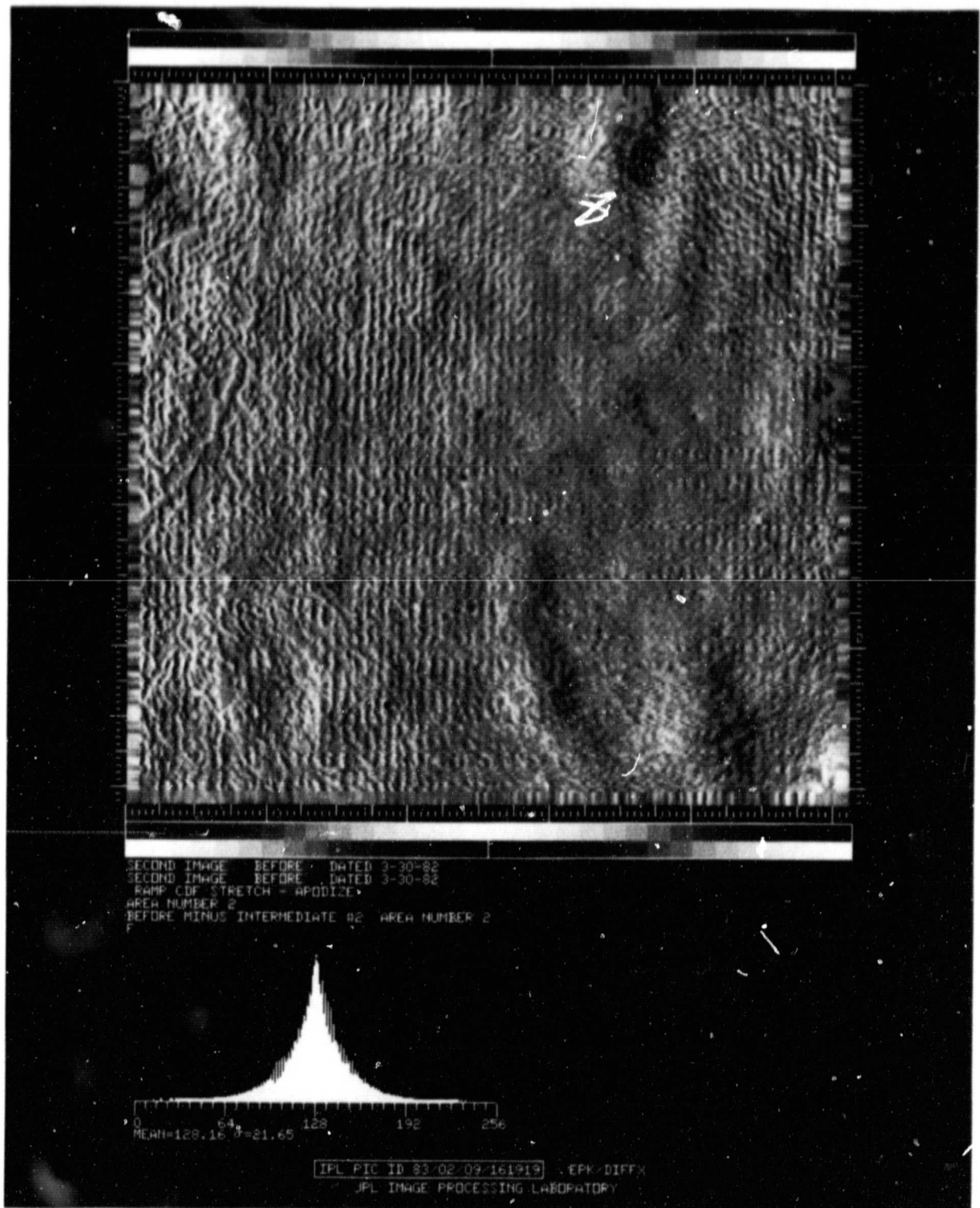


Figure 8b. Enhanced Difference Image of Sheet B Subarea 2, Before-Intermediate #2

while stretching would be expected to increase with time.) Figure 9 shows the before-after image for sheet C.

Therefore, although the FFTs do not reveal any micro-burnishing, it appears that the other type of degradation of concern, that of stressing, does occur in sheet B. This would indicate that the plexiglas does not provide a perfect environmental barrier, but rather allows the micro-climate inside the plexiglas to respond to exterior changes in the environment, which places stress on the sheet. It should be noted that prior to raking-light photography, the sheets were allowed to equilibrate to room conditions each time, but did not return to their original, unstressed state.

ORIGINAL PAGE IS  
OF POOR QUALITY

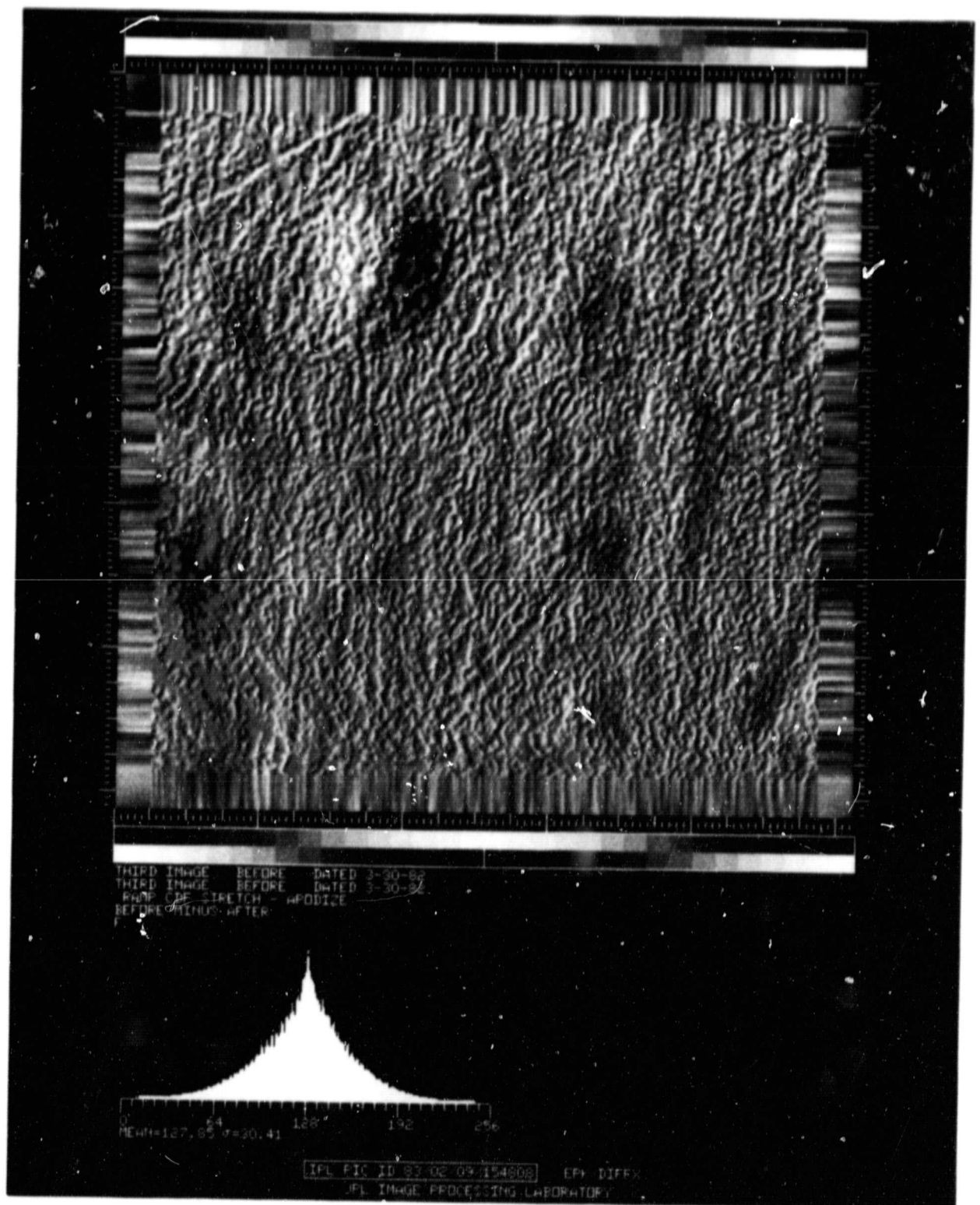


Figure 9. Enhanced Difference Image of Sheet C, Before - After

#### 4.0 CONCLUSION

In conclusion, two types of degradation were found for the Codex simulation. The first was a consistent decrease with time of the amplitude of the mesoscale deformations, with sizes in the 8mm range. These changes are of no concern. No micro-burnishing was detected. The second degradation that appeared to occur was a differential stretching of the simulation sheet, which increased with time. This degradation is of concern, and indicates that the encapsulation technique used for the Codex Hammer probably does not completely isolate it from its environment. The relation of the environmental test conditions to those to which the Codex is exposed and the applicability of this accelerated life test to the Codex itself are to be determined by LACMA.

ORIGINAL PAGE IS  
OF POOR QUALITY

Table 1.

JPL Photolab Numbers for Figures

<u>Figure No.</u>	<u>JPL Photolab No.</u>
1a	M4207B
b	M4207A
c	M4208B
d	M4208A
e	M4209A
f	M4209B
g	M4210B
h	M4210A
2a	M4211A
b	M4211B
c	M4213B
d	M4213A
6	M4214B
7a	M4214A
b	M4215B
8a	M4215A
b	M4212B
9	M4212A

## REFERENCES

Armand Hammer Foundation, 1981. "The Codex Hammer by Leonardo da Vinci", exhibit brochure.